Multi-Machine Determination of SOL-to-Core Multi-Z Impurity Transport in Advanced Confinement Regimes

N. Howard[1*], T. Abrams[2], F. Scotti[3], B. Grierson[4], A. Jarvinen[3], T. Odstrcil[2], F. Sciortino[1], W. Guttenfelder[4], B. Victor[3], S. Haskey[4], J. Nichols[5], S. Zamperini[5], A. Bortolon[4], F. Effenberg[4]

[1]MIT Plasma Science and Fusion Center, Cambridge, Massachusetts, USA

[2]General Atomics, San Diego, California, USA

[3]Lawrence Livermore National Lab, Livermore, California, USA

[4]Princeton Plasma Physics Lab, Princeton, New Jersey, USA

[5]University of Tennessee - Knoxville, Knoxville, Tennessee, USA

*email: nthoward@psfc.mit.edu

As the world fusion program forges into the burning plasma era, it is clear that the successful operation of a burning plasma will require conditions that simultaneously balance the needs of the power exhaust challenge with a high performance pedestal and minimal core impurity accumulation. The interconnected nature of impurity transport demands a robust, integrated understanding of impurity sources and transport that can only be derived from multi-machine, core to edge investigation of impurities. As part of the FY20 Joint Research Target, 8 datasets obtained from 3 US tokamaks (Alcator C-Mod, DIII-D, and NSTX/NSTX-U) were used to perform coordinated research to study impurities from generation at material interfaces to their eventual accumulation in the core. This analysis validated state-of-the-art SOL modeling that demonstrates near-SOL impurity accumulation, explained the role of impurity ionization and neoclassical transport in the recovery of high performance pedestals, validated gyrokinetic impurity transport predictions across 3 devices, and demonstrated the ability of ECH to eliminate core impurity accumulation, independent of Z and advanced confinement regime.

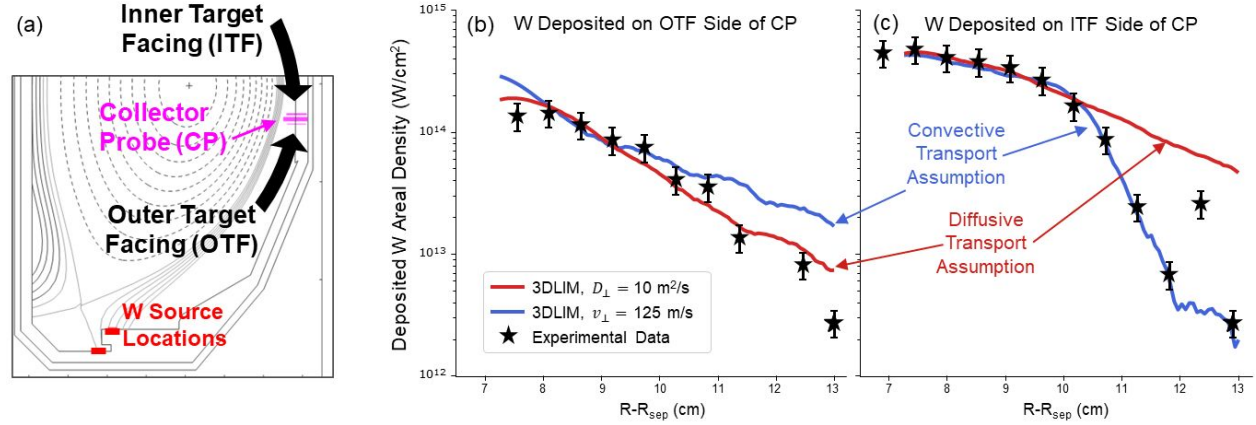

Figure 1. (a) Diagram of the experimental midplane collector probe setup for the far-SOL high-Z impurity transport experiment in DIII-D. (b)-(c): Experimental (symbols) and calculated (solid lines) W deposition profiles on the (b) OTF and (c) ITF sides of the midplane CP. The modeling uses the 3DLIM code assuming either purely diffusive (red) or purely convective (blue) radial W transport and is normalized to experiment.

Collector probe measurements were used to validate state-of-the-art simulations illustrating the role of convective transport in explaining near-SOL impurity accumulation. Data obtained in LSN discharges only differing in the B×∇B drift direction were interpreted by 3DLIM, a new 3D Monte Carlo far-SOL impurity transport code. Probe results were consistent with the long-hypothesized near-SOL impurity

accumulation in the inner target facing (ITF) direction, which modeling suggests may only form when the ∇B direction is away from the active divertor, due to the presence of fast parallel SOL flows when the ∇B direction is towards the divertor. Interpretive modeling assuming purely diffusive radial transport (10 m^2/s) yields reasonable agreement with experimental measurements of W deposition on the outer-target facing (OTF) sides of the probe (Figure 1), while failing to reproduce the inner-target facing direction. In contrast, a purely convective radial transport model (125 m/s radially outwards) is shown to simultaneously agree with both sides of the collector probe's deposition profiles - indicating a potentially dominant role of non-diffusive process in the SOL independent of the ∇B direction studied and representing the most convincing evidence of near SOL accumulation to date. Also on DIII-D, in-situ spectroscopic measurements of W on were collected on DIII-D that show that near the outer strike point, net and gross erosion of tungsten are nearly equal for conditions where the W ionization length is large compared with its gyro-radius ($l_W >> \rho_W$). These results were found to be well reproduced by analytic models. In contrast, as l_W decreases, the rate at which tungsten net erosion also decreases relative to W gross erosion, is somewhat reproduced by a recently developed model which relates W net erosion to the ratio of l_W and width of the magnetic pre-sheath, indicating the importance of electric field effects in regulating prompt re-deposition in addition to gyro-motion. As the spectroscopic measurements only account for re-deposition from W^+, it is concluded that re-deposition from charge states higher than W^+ is likely also important in regulating the balance between high-Z sourcing, leakage, and re-deposition.

The first 3D edge modeling of boron impurity transport in DIII-D was also performed, and found that changes in the balance of parallel friction forces in the SOL alter spatial boron distributions as a function of upstream plasma density. EMC3-EIRENE simulations of impurity powder dropper experiments indicate that high density operation favors boron fluxes directly to the inner target, while low plasma density favors a more uniform B distribution. Simulations using a localized source of boron atoms also indicate that the boron flux to the divertor surface demonstrates significant toroidal asymmetries, as measured directly in experiments. However, the simulated spatial scales are not compatible with the striations observed, indicating this effect cannot be entirely ascribed to the source localization and that uncompensated error fields also play a key role.

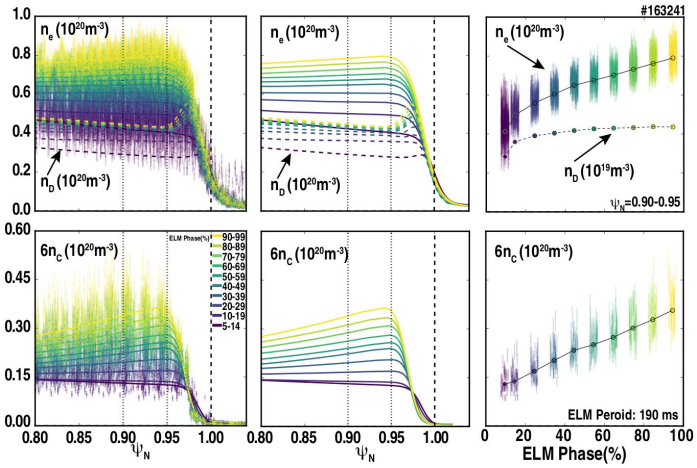

Figure 2: ELM phase synchronized analysis of the pedestal recovery over 3.0 seconds of quasi-stationary conditions shown in space with (left) data and fits, (middle) fits only and (right) time evolution at top of pedestal. ELM phase has been divided into 10 segments and reveals dominance of carbon fueling beyond 20% into ELM cycle.

Direct measurements of main-ions identified the role of ionization and neoclassical impurity transport in the pedestal. Using charge exchange, coupled with measured electron and fully-stripped carbon densities, were able to unveil the dynamics of inter-ELM evolution (Figure 2). Inter-ELM evolution was found to occur in two phases: (i) rapid initial recovery of main-ion and electron density followed by (ii) slower impurity and electron density buildup with primarily impurity fueling. A significant fraction of the electron density recovery can be directly attributed to impurity ionization and influx. The temporal dynamics of this process were modeled using the STRAHL code, and are consistent with the establishment of an neoclassically driven impurity pinch early in the ELM cycle, which preferentially favors inward impurity transport over main-ion fueling in these conditions. By flattening the electron and main-ion density (by reduced recycling or increased opacity) it is predicted that the inward impurity pinch can be reduced, eliminated, or even reversed. The findings are largely consistent with results from both NSTX, NSTX-U and C-Mod, indicating the robust nature of the results.

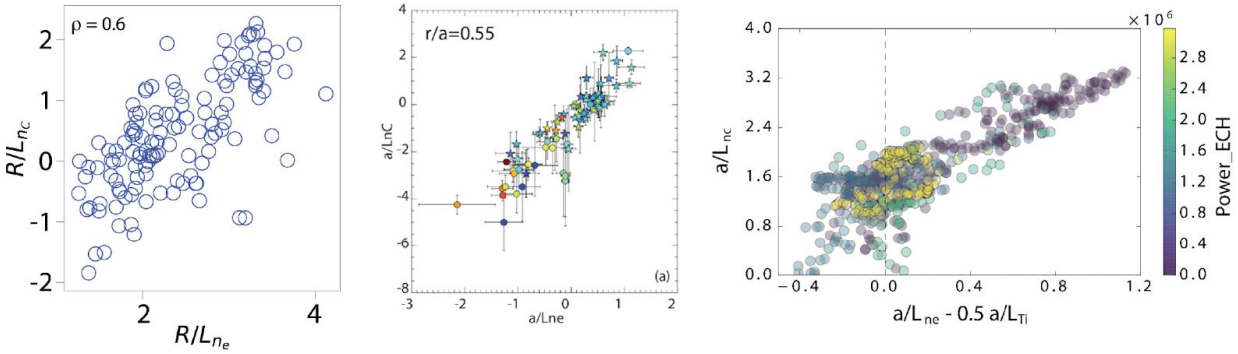

Figure 3. (left) DIII-D and (middle) NSTX database shown R/L_{nz} versus R/L_{ne} (right) scatter plot showing measured impurity peaking versus the neoclassical peaking proxy colored by ECH heating

Four cross machine datasets (Alcator C-Mod, DIII-D, NSTX/U) were used to validate leading transport models and establish actuators for the regulation of core impurity accumulation in a wide range of plasma conditions. DIII-D's unique neutral beam configurations were leveraged to break typical correlations between rotation and other plasma parameters, enabling a novel investigation into the role of rotodiffusion in determining impurity peaking. In contrast to previous work on JET and ASDEX, the DIII-D results indicate a negligible role of rotodiffusion and suggest that a balance of other pinch contributions likely explain DIII-D impurity peaking. Multi-machine comparisons were able to identify robust conclusions about the physical origin of core impurity transport. Near-axis transport is in good quantitative agreement with NEO calculations nearly independent of both the regime and machine studied, whereas transport outside of mid-radius appears turbulent in nature. A study of three large databases revealed correlations with turbulent and neoclassical transport drives, including a robust peaking of impurities correlated with peaked electron density. Linear and nonlinear gyrokinetic modeling (CGYRO) yields generally reasonable agreement with experiment but points to regions of parameter space where the origin of measured impurity transport is still not well understood. Using a dataset that captured a wide range of advanced operating scenarios on DIII-D (high q-min, hybrids, QH-modes, etc.), it was shown that a proxy for neoclassical peaking/screening ($a/L_{n,e}$ - 0.5 a/L_{Ti}) was an effective indicator of peaking independent of both the operational regime and impurity charge, and a modest (~1.0 MW) Electron Cyclotron Heating was capable of reducing or eliminating peaked profiles. These results increase confidence in our ability to predict transport and control impurity buildup with central electron heating in future burning plasmas.